Use of Pressure Derivative in Well-Test Interpretation

Dominique Bourdet,* SPE, **J.A. Ayoub,** SPE, and **Y.M. Pirard,**** SPE, Flopetrol-Johnston Schlumberger

Summary. A well-test interpretation method based on the analysis of the time rate of pressure change and the actual pressure response is discussed. A differentiation algorithm is proposed, and several field examples illustrate how the method simplifies the analysis process, making interpretation of well tests easier and more accurate.

Introduction

The interpretation of pressure data recorded during a well test has been used for many years to evaluate reservoir characteristics. Static reservoir pressure, measured in shut-in wells, is used to predict reserves in place through material-balance calculations. Transient-pressure analysis provides a description of the reservoir flowing behavior. Many methods have been proposed for interpretation of transient tests,[1] but the best known and most widely used is Horner's.[2] More recently, type curves, which indicate the pressure response of flowing wells under a variety of well and reservoir configurations, were introduced.[3-8] Comparison of transient-pressure measurements with type curves provides the only reliable means for identifying that portion of the pressure data that can be analyzed by conventional straight-line analysis methods.

Recently, the quality of well-test interpretations has improved considerably because of the availability of accurate pressure data (from electronic pressure gauges) and the development of new software for computer-aided analysis. An increasing number of theoretical interpretation models that allow a more detailed definition of the flow behavior in the producing formation are now in use.

Surprisingly, the commonly used analysis techniques have not followed the general progress evident in hardware and in interpretation models, making the interpretation procedure complicated and time-consuming. Type curves are seen by various analysts as overly simplistic or overly complex, difficult to distinguish, and/or cumbersome to use. Yet, mere identification of straight lines on a pressure-vs.-time graph is a "ruler approach"—convenient for hand analysis but ignoring powerful computing facilities that are available. Furthermore, the conventional straight-line analysis methods fail to use all the data available and can result in significant errors.

We propose an interpretation method based on the analysis of the derivative of pressure with respect to the appropriate time function—natural logarithm of time or Horner/superposition time functions. This method considers the response as a whole, from very-early-time data to the last recorded point, and uses the type-curve-matching technique. It provides a description of the flow behavior in the reservoir, but with the logarithmic derivative, it also emphasizes the infinite radial flow regime, of prime interest in well-test interpretation. The approach is an extension of the Horner method to analyze the global response with improved definition.

Use of the derivative of pressure vs. time is mathematically satisfying because the derivative is directly represented in one term of the diffusivity equation, which is the governing equation for the models of transient-pressure behavior used in well-test analysis. Thus, the derivative response is more sensitive to small phenomena of interest that are integrated and hence diminished by the pressure-vs.-time solutions.

One limitation of the pressure derivative in analysis is the difficulty in collecting differentiable pressure-transient data. Accurate and frequent pressure measurements are required. However, pressure measurement and the computer processing technologies now available at wellsites allow pressure-derivative analysis.

The pressure-derivative method is demonstrated for a homogeneous reservoir and compared with conventional interpretation techniques. The practical aspects of differentiation of actual pressure data are discussed. Application of the derivative analysis to heterogeneous formations reveals the good definition obtained with derivative plots, and the distinction between currently used interpretation models is clearly shown.

*Now with Kappa Engineering.
**Now a consultant.

Copyright 1989 Society of Petroleum Engineers

Transient-Pressure Analysis Applied to Homogeneous Reservoirs

Conventional well-test interpretation has focused on the homogeneous reservoir solution. The corresponding pressure-analysis methods have been discussed extensively in the literature and are commonly used.

Two complementary approaches are used for transient-pressure analysis: (1) a global approach is used to diagnose the pressure behavior and to identify the various characteristic flow regimes, and (2) specialized analyses, valid only for specific flow regimes, are performed on selected portions of the pressure data. Results of analyses with both approaches must be consistent.

Diagnosis of pressure behavior is performed by type-curve analysis. Fig. 1 describes a well with wellbore storage and skin in a reservoir with homogeneous behavior.[5] Dimensionless pressure, p_D, is plotted on log-log scale vs. dimensionless time group, t_D/C_D. The resultant curves, characterized by the dimensionless group C_De^{2S} (Appendix A of Ref. 9), correspond to well conditions ranging from damaged wells to acidized and fractured wells.

Two flow regimes of interest can be identified in the pressure response (Fig. 1). At early time, all the curves merge to an asymptote of slope equal to unity, corresponding to pure wellbore-storage effect given by

$$p_D=t_D/C_D. \quad \ldots\ldots\ldots\

TABLE 1—PRESSURE vs. ELAPSED TIME, BUILDUP 2

Elapsed Time (hours)	Pressure Change (psi)	Pressure Derivative $L=0.0$	Pressure Derivative $L=0.1$	Superposition Time (hours)
0.00417	0.57000	4.67619	4.67619	−8.21072
0.00833	3.81000	5.99244	5.99244	−7.51785
0.01250	6.55000	9.88966	9.88966	−7.11265
0.01667	10.03000	13.47654	13.47654	−6.82524
0.02083	13.27000	17.11777	17.11777	−6.60237
0.02500	16.77000	20.21677	20.21677	−6.42032
0.02917	20.01000	22.80169	22.80169	−6.26644
0.03333	23.25000	26.04514	26.04514	−6.13318
0.03750	26.49000	22.89854	22.89854	−6.01567
0.04583	29.48000	28.64550	26.07281	−5.81554
0.05000	32.48000	37.32830	34.75561	−5.72880
0.05833	38.96000	47.62447	47.62477	−5.57519
0.06667	45.92000	48.31909	48.31909	−5.44220
0.07500	51.17000	53.72652	53.72652	−5.32496
0.08333	57.64000	79.46690	79.46690	−5.22014
0.09583	71.95000	86.30312	86.30312	−5.08119
0.10833	80.68000	71.39044	71.39044	−4.95940
0.12083	88.39000	80.75224	76.23615	−4.85101
0.13333	97.12000	84.57822	88.17867	−4.75338
0.14583	104.24000	93.41637	100.49477	−4.66457
0.16250	115.96000	110.24378	112.88589	−4.55743
0.17917	126.68000	119.68448	120.33011	−4.46087
0.19583	137.89000	128.84697	128.52133	−4.37300
0.21250	148.37000	137.15276	137.73179	−4.29239
0.22917	159.07000	145.94349	146.17935	−4.21795
0.25000	171.79000	155.45732	157.33866	−4.13228
0.29167	197.12000	171.82610	171.82610	−3.98080
0.33333	220.15000	193.82046	193.82046	−3.84994
0.37500	244.34000	211.90679	211.90679	−3.73481
0.41667	266.27000	207.41087	214.27465	−3.63209
0.45833	284.98000	216.94507	225.81104	−3.53943
0.50000	304.44000	241.44644	242.18326	−3.45505
0.54167	323.90000	265.63388	244.41899	−3.37764
0.58333	343.83000	245.32062	258.20507	−3.30615
0.62500	358.05000	255.51098	266.46221	−3.23978
0.66667	376.26000	282.01815	247.89436	−3.17784
0.70833	391.97000	241.91919	281.65393	−3.11982
0.75000	403.69000	261.81605	267.33064	−3.06526
0.81250	428.63000	295.67097	269.37561	−2.98909
0.87500	447.34000	257.26690	284.85072	−2.91885
0.93750	463.55000	275.22503	268.73064	−2.85371
1.00000	481.75000	276.61744	278.65451	−2.79300
1.06250	496.23000	285.06295	290.20879	−2.73620
1.12500	512.95000	300.11545	275.48309	−2.68285
1.18750	527.41000	288.40871	283.97748	−2.63257
1.25000	541.15000	251.41519	276.06601	−2.58505
1.31250	550.86000	248.81673	267.54944	−2.54003
1.37500	562.85000	281.02901	260.53933	−2.49725
1.43750	574.32000	262.57879	254.14388	−2.45654
1.50000	583.81000	247.74806	249.77847	−2.41770
1.62500	602.27000	225.11828	231.84295	−2.34505
1.75000	615.52000	211.05283	225.84044	−2.27829
1.87500	629.26000	224.58855	200.91071	−2.21659
2.00000	642.23000	205.89532	194.76486	−2.15929

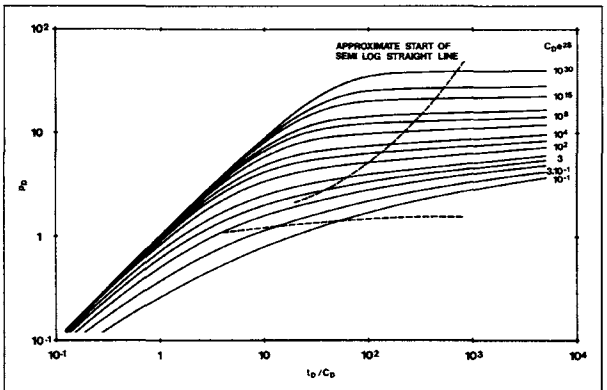

Fig. 1—Wellbore-storage and skin type curves for a homogeneous reservoir.[5]

TABLE 1—PRESSURE vs. ELAPSED TIME, BUILDUP 2 (continued)

Elapsed Time (hours)	Pressure Change (psi)	Pressure Derivative $L=0.0$	Pressure Derivative $L=0.1$	Superposition Time (hours)
2.25000	659.71000	162.25279	159.78026	−2.05583
2.37500	667.19000	149.94510	151.22713	−2.00885
2.50000	673.44000	139.99198	149.04678	−1.96459
2.75000	684.65000	140.37167	138.91767	−1.88321
3.00000	695.11000	138.47093	126.58152	−1.80993
3.25000	704.06000	113.73940	135.38378	−1.74343
3.50000	709.80000	135.84157	134.55333	−1.68269
3.75000	719.50000	148.73954	111.93829	−1.62688
4.00000	725.97000	106.36197	109.31883	−1.57536
4.25000	730.20000	63.06567	86.38834	−1.52759
4.50000	731.95000	40.78765	75.31986	−1.48312
4.75000	733.70000	56.85782	70.70269	−1.44158
5.00000	736.45000	79.90940	66.24425	−1.40266
5.25000	739.69000	87.07801	69.37689	−1.36609
5.50000	742.64000	74.17246	62.20195	−1.33165
5.75000	744.70000	72.37656	55.61930	−1.29912
6.00000	747.19000	70.17938	53.35277	−1.26836
6.25000	748.94000	33.00165	42.51997	−1.23919
6.75000	748.02000	21.38772	37.84478	−1.18513
7.25000	750.78000	52.87202	29.90081	−1.13606
7.75000	753.01000	42.98848	34.27710	−1.09127
8.25000	754.52000	41.68190	42.43457	−1.05019
8.75000	756.27000	40.60712	39.99428	−1.01233
9.25000	757.51000	33.15981	37.85081	−0.97731
9.75000	758.52000	40.47033	37.11028	−0.94480
10.25000	760.01000	37.30584	36.78727	−0.91453
10.75000	760.75000	32.36145	36.16443	−0.88626
11.25000	761.76000	33.83440	34.92720	−0.85979
11.75000	762.50000	36.69708	35.73146	−0.83494
12.25000	763.51000	38.24900	33.19398	−0.81156
12.75000	764.25000	36.56733	32.83639	−0.78953
13.25000	765.07000	30.36816	33.82743	−0.76871
13.75000	765.50000	27.79694	33.49276	−0.74901
14.50000	766.50000	32.60263	33.22815	−0.72137
15.25000	767.25000	30.24218	32.87881	−0.69577
16.00000	767.99000	32.53602	31.30233	−0.67199
16.75000	768.74000	34.84104	31.89127	−0.64983
17.50000	769.48000	30.88607	32.05207	−0.62914
18.25000	769.99000	33.73485	31.26438	−0.60977
19.00000	770.73000	27.55673	30.18581	−0.59158
19.75000	770.99000	23.34734	30.37291	−0.57448
20.50000	771.49000	40.41950	29.85512	−0.55836
21.25000	772.24000	39.06894	29.75090	−0.54314
22.25000	772.74000	26.72085	28.67977	−0.52413
23.25000	773.22000	21.23086	28.48296	−0.50643
24.25000	773.48000	24.65156	28.54120	−0.48991
25.25000	773.99000	33.76653	28.71951	−0.47445
26.25000	774.49000	25.79328	26.18140	−0.45995
27.25000	774.73000	23.98014	31.10344	−0.44633
28.50000	775.23000	31.41352	26.52348	−0.43041

Flow History

t_p, hours	15.33
q, STB/D	174

Well and Reservoir Parameters

B	1.06
c_t, psi^{-1}	4.2×10^{-6}
h, ft	107
ϕ	0.25
μ, cp	2.5
r_w, ft	0.29

In this example, the analyzed data were recorded during buildup. A semilog straight line could develop (Fig. 3) because the data are corrected for buildup effect with the Horner method. A correction should also be performed for the log-log analysis because the type curves of Fig. 1 are designed to describe drawdowns.

Fig. 4 illustrates the pressure response during an "ideal" test. The well, first at initial pressure, p_i, is opened and produced at constant rate during t_p. Then it is closed for buildup, and after infinite shut-in time, the pressure will be back at p_i (if the system behavior is infinite-acting). In terms of pressure change, it will then

Downloaded from http://onepetro.org/FE/article-pdf/4/02/293/2630137/spe-12777-pa.pdf/1 by Sandia National Laboratories user on 04 June 2025

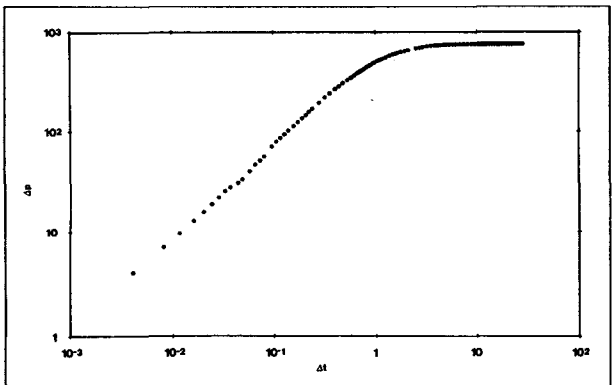

Fig. 2—A diagnostic tool: log-log plot of buildup data.

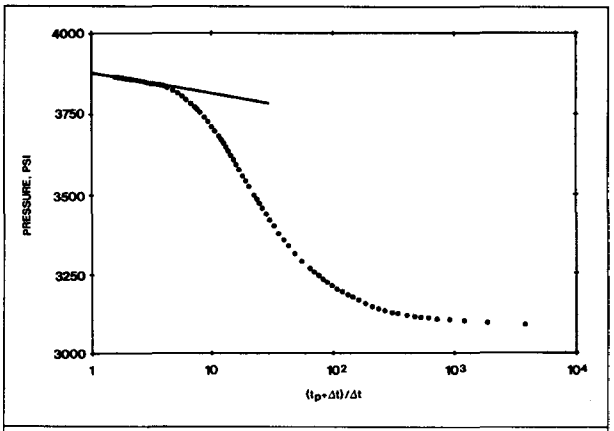

Fig. 3—Horner plot.

take an infinite shut-in time to reach a Δp_{BU} of the same amplitude as the pressure drop at the end of the drawdown $\Delta p_{Dd}(t_p)$. As a result, drawdown and buildup curves are not identical. In Fig. 5, the dotted line corresponds to a drawdown type curve. After the well is shut in at t_p, the resulting buildup response (thick line) deviates from the drawdown type curve and flattens toward the same level as the last drawdown-pressure change before shut-in, $\Delta p_{Dd}(t_p)$. This deviation is more pronounced when the flow time before shut-in is relatively short, as is often the case when exploration wells are tested.

In practice, it is not possible to ascertain a perfectly constant flow rate during drawdown, especially during the initial instants of flow. Log-log analysis considers the global response during a flow period and therefore does not accommodate any rate variation during the period analyzed. As a result, only buildups, recorded on shut-in wells, generally are suitable for type-curve matching. When the interpretation is performed on computer, the buildup type curve is generated for the actual flow history before shut-in (multirate curves):

$$p_D=\sum_{i=1}^{n-1}[(q_i-q_{i-1})/(q_{n-1}-q_n)]\left[p_D\left(\sum_{j=1}^{n-1}\Delta t_{jD}\right)-p_D\left(\sum_{j=i}^{n-1}\Delta t_{jD}+\Delta t_D\right)\right]+p_D(\Delta t_D), \quad \ldots\ldots\ldots\ldots (3)$$

and the match is performed on the exact theoretical response. Recently published examples show this may become crucial.[11]

Derivative of Pressure

Fig. 6 represents the same response as in Fig. 1 but with the semilog slope of the dimensionless pressure response on the y axis, vs. the usual dimensionless time group t_D/C_D on the x axis.[10] The curves are generated by taking the derivative of the pressure with respect to the natural logarithm of time.

$$dp_D/[d\ \ln(t_D/C_D)]=(t_D/C_D)\{dp_D/[d(t_D/C_D)]\}=(t_D/C_D)p'_D. \quad \ldots\ldots\ldots\ldots\ldots\ldots\ldots\ldots\ldots\ldots (4)$$

The first typical regime observed on the type curve of Fig. 1 is wellbore-storage effect. By combining Eqs. 1 and 4, we obtain

$$(t_D/C_D)p'_D=t_D/C_D. \quad \ldots\ldots\ldots\ldots\ldots\ldots\ldots\ldots\ldots\ldots\ldots\ldots (5)$$

As for pressure, all the derivative behaviors are identical at early time, and the curves merge on a single asymptote of slope equal to unity.

When the infinite-acting radial flow regime has been reached—i.e., after the limit "approximate start of the semilog straight line" (Fig. 1)—the pressure behavior is described by Eq. 2. The semilog slope is constant:

$$(t_D/C_D)p'_D=0.5, \quad \ldots\ldots\ldots\ldots\ldots\ldots\ldots\ldots\ldots\ldots\ldots\ldots (6)$$

and all the derivative curves merge to a second asymptote, the one-half straight line. Because the infinite-acting radial flow produces a characteristic straight line on log-log scale, the derivative plot can be used in place of the conventional semilog pressure plot for the accurate determination of kh/μ.

Between the two asymptotes, and depending on the C_De^{2S} group, each curve shows a specific shape much more pronounced than that of the usual pressure curves (Fig. 1). Therefore, the derivative method is powerful for diagnosis and, in fact, it combines on the same log-log plot the global approach by type curves and the accurate specialized analysis of radial flow. Thus, there is no need for refinements; the match is direct, simplifying the analysis process. Provided that the data show wellbore storage and infinite-acting radial flow regimes, the match is unique because of unique behavior at both ends. The curve match is obtained by identification of the

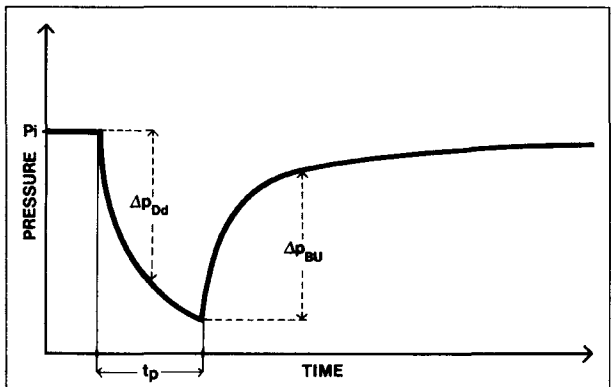

Fig. 4—Pressure history of a simple drawdown/buildup test.

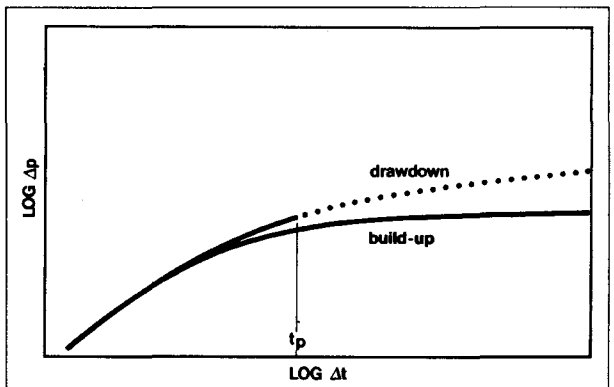

Fig. 5—Drawdown and buildup type curves.

Downloaded from http://onepetro.org/FE/article-pdf/4/02/293/2630137/spe-12777-pa.pdf/1 by Sandia National Laboratories user on 04 June 2025

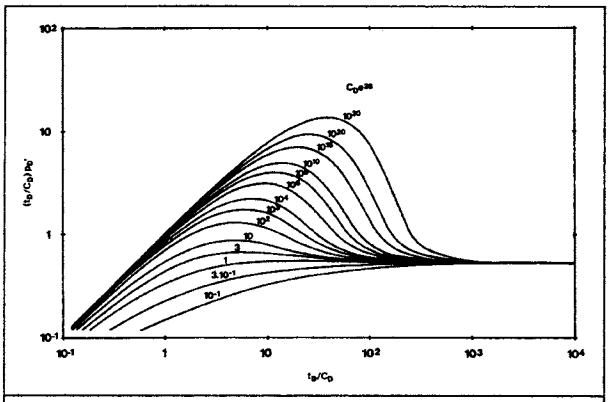

Fig. 6—Derivative type curve for homogeneous reservoir.[10]

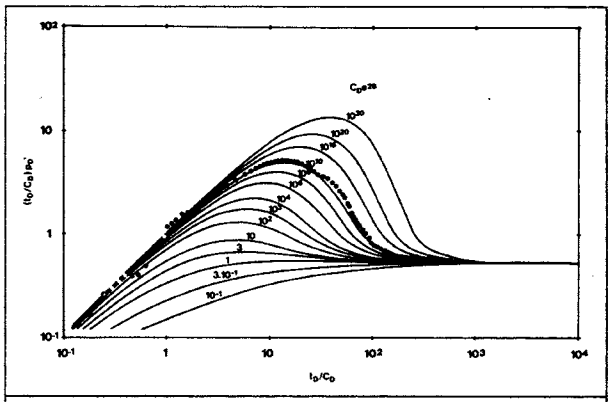

Fig. 7—Match of the derivative of actual data.

curve following the data at intermediate time between the two asymptotes.

For buildup analysis, the same curves were found to be applicable (Ref. 10) provided that the derivative is taken, not with respect to natural logarithm of time, but with respect to natural logarithm of the Horner time, as modified by Agarwal[12]:

$$dp/\{d\ \ln[t_p\Delta t/(t_p+\Delta t)]\}=\Delta t[(t_p+\Delta t)/t_p](dp/dt). \quad \ldots\ldots\ (7)$$

These buildup derivative responses, when plotted vs. the actual shut-in time, Δt, match on the type curve of Fig. 6. This behavior is present when the Horner method is valid—i.e., the drawdown has to reach radial flow before shut-in.

Fig. 7 presents the slope of the example Horner plot (Fig. 3), plotted on a log-log scale vs. shut-in time. The matching procedure on the type curve of Fig. 6 is as follows.

1. The constant-derivative part of the data plot is placed on the one-half straight line of the type curve. The pressure match is then fixed accurately and kh/μ is known.

2. The data plot is displaced along the one-half straight line until wellbore-storage data match on the early-time unit-slope asymptote of the type curve. The time match is now fixed, yielding the wellbore-storage constant, C.

3. A direct reading tells which C_De^{2S} curve provides the best match between the two asymptotes, giving access to the skin factor, S.

Experience has shown that for practical reasons discussed later with the differentiation of actual data, it is convenient to match both pressure and pressure-derivative curves, even though it is redundant.[10] With the double match, a higher degree of confidence in the results is obtained. To illustrate this, the final match of the example in Table 1 is shown in Fig. 8.

The skin coefficient is no longer present on derivative responses when the infinite-acting radial flow configuration is reached (on the one-half line), and as a result, S can be estimated from only the derivative C_De^{2S} match during the transition between the two asymptotic regimes. This property of the derivative presents, in some cases, interesting features for the interpreter. For example, when a well is tested before and after stimulation, if the well treatment has not modified the characteristics of the producing zones, derivative behaviors recorded during both tests should match exactly when the data curves are free of any wellbore-storage effect. The limited influence of the skin coefficient on derivative responses will be of interest for the analysis of heterogeneous formations and for the identification of boundary effects. As discussed later, the traditional flow regimes produce a characteristic shape much faster than on the usual pressure curves.

Other applications of the derivative of pressure have been proposed for observation wells[13] and fractured wells[14] that use the derivative of pressure with respect to elapsed time. In the method presented here, it is preferable to consider the derivative as the semilog (or Horner/superposition) slope for the following reasons:

1. The semilog derivative emphasizes the infinite-acting radial flow regime of prime interest in well-test interpretation.

2. When the derivative is considered as the slope of the semilog or the superposition plot, both the pressure change and the pressure derivative are made dimensionless by use of the same group ($kh/141.2qB\mu$ in usual oilfield units), making the double match practical.

3. The derivative with respect to the Horner/superposition function converts buildup analysis to that of drawdown, simplifying the analysis process.

4. Buildup analysis reveals an additional advantage in the use of the Horner/superposition derivative of pressure: the resulting curves are neither compressed on the time axis, as for traditional Horner/superposition analysis, nor on the pressure axis, as for buildup pressure type curves. The derivative displays the full amplitude of the signal and therefore improves the sensitivity of the analysis plots.

5. The noise apparent in the derivative data can be reduced when the superposition function is used because the slope (and the derivative) will not tend toward zero during the infinite-acting period.

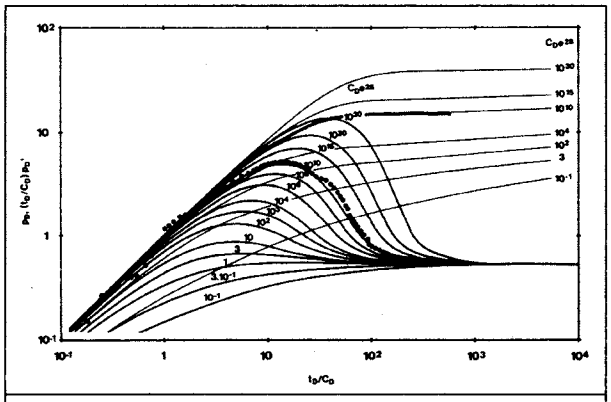

Fig. 8—The combined match.

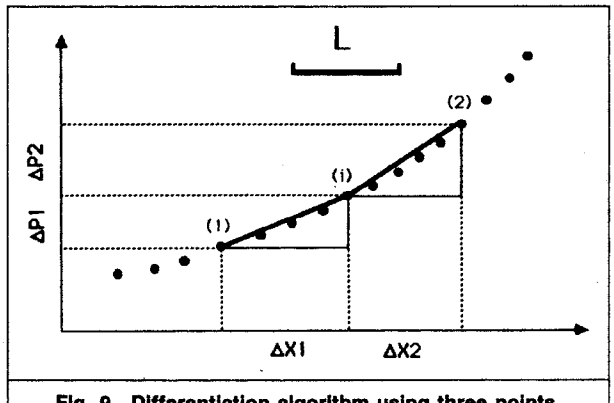

Fig. 9—Differentiation algorithm using three points.

Downloaded from http://onepetro.org/FE/article-pdf/4/02/293/2630137/spe-12777-pa.pdf/1 by Sandia National Laboratories user on 04 June 2025

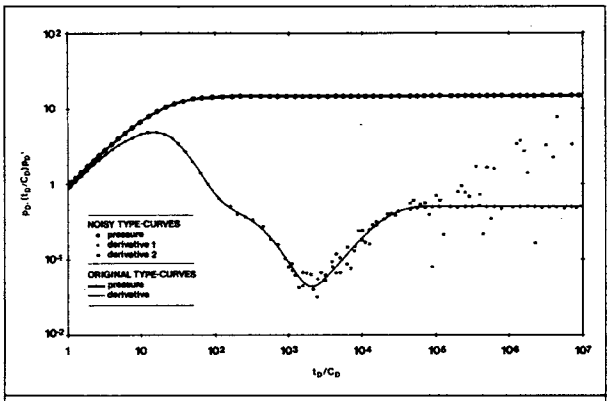

Fig. 10—Test of the differentiation algorithm on noisy data.

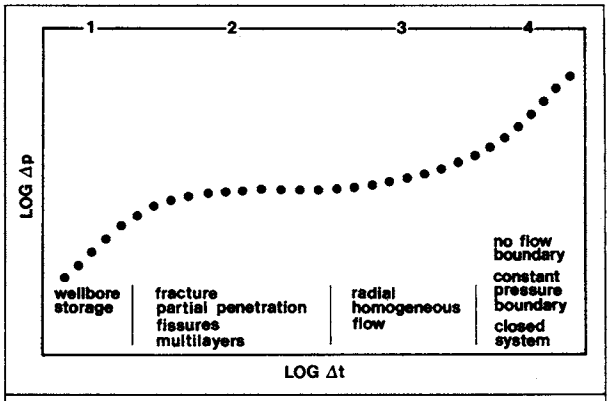

Fig. 11—Log-log plot of a typical drawdown.

Differentiation Algorithm

The main concern when actual data are being differentiated is to improve the signal-to-noise ratio. Some noise will always be present because of gauge resolution, electronic circuitry, vibrations, etc. Differentiation is difficult, if not inconclusive, for the relatively high noise level associated with a low sampling rate. This is frequently the case with mechanical gauges, which also produce noise on both pressure and time axes.

Several approaches for differentiating data have been tried (Appendix B). Because the correct result is not known when working with actual data, modified type curves were used to evaluate the different methods. A random noise both proportional to and independent of the amplitude of the p_D signal was added to the type curve, and the number of points generating the p_D curve was reduced by a random sampling process.

Preferred Algorithm. The algorithm presented here is simple, and is the best adapted to test interpretation needs. This differentiation algorithm reproduces the test type curve over the complete time interval better than others. It uses one point before and one point after the point of interest, i, calculates the corresponding derivatives, and places their weighted mean at the point considered (Fig. 9).

$$(dp/dX)_i=[(\Delta p_1/\Delta X_1)\Delta X_2+(\Delta p_2/\Delta X_2)\Delta X_1]/(\Delta X_1+\Delta X_2), \quad \ldots\ldots\ldots\

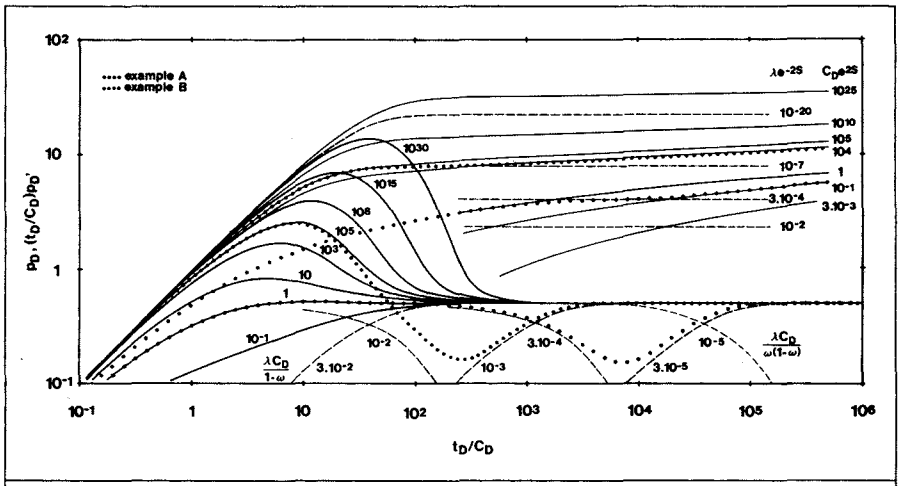

Fig. 12—Derivative type curve for double-porosity reservoir (pseudosteady-state blocks to fissure flow).[17]

When the complete recommended procedure is used, the distortions produced by the differentiation algorithm presented here are practically independent of the point density in the curve. The same effect is expected to be produced on both data and theoretical curves, as opposed to the algorithms that use all the points present in a given time interval for smoothing.

Some of the irregularities observed in the derivative behavior were found to be part of the reservoir response. For example, oscillations of pressure caused by tidal effects are emphasized by the derivative at late time, when the signal is barely changing.

Another advantage is that the derivative would still give results when the last flowing pressure is missing, as when the gauge is run after shut-in or in some cases of changing wellbore storage. The $p(\Delta t=0)$ point is not needed to produce the derivative curve; thus, provided that enough data are available, a unique match is possible and the skin is accessible. The derivative plots also tend to compensate starting-time errors encountered when shut-in time is not accurate enough compared with the pressure-gauge sampling frequency. In addition, for gas wells, the differential of the real gas potential $m(p)$[15] replaces the calculation of an integral by that of a product.

$$dm(p)/d\ln(\Delta t)=\{2p/[\mu(p)z(p)]\}\Delta t\Delta p'. \quad \ldots\ldots\ldots\ldots (10)$$

Application to Heterogeneous Reservoir Bathing

Recent theoretical developments and related publications demonstrate a general oil industry interest in the behavior of heterogeneous formations. In fact, it is our experience, based on a very large number of well tests, that in some areas, up to 30 or 40% of the wells show a heterogeneous behavior. This is evident when high-accuracy pressure data, high-definition analysis techniques such as plots of the derivative of pressure, and computer-aided interpretation are used. The combined recent progress in data acquisition, data processing, and computing techniques offers new prospects for the interpretation of well-test data. Much more information is pulled out of the well during today's tests. Interpretation should make full use of all data available for analysis.

Fig. 11 presents a typical drawdown log-log plot of Δp vs. Δt. Four different time periods can be identified in the pressure response.

1. The wellbore-storage effect is always the first flow regime to appear.
2. Evidence of well and reservoir heterogeneities then may follow. Such behavior may be a result of the effects of a fractured well, a partially penetrating well, a fissured formation, or a multilayered reservoir.
3. After some production time, the system starts to exhibit a radial flow behavior, representing an equivalent homogeneous system composed of all producing elements.
4. Boundary effects may occur at late time.

Thus, many types of flow regimes can appear before (and after) the actual semilog straight line develops, and they follow a very strict chronology in the pressure response. Only a global diagnosis, with identification of all successive regimes present, will indicate exactly when conventional analysis, like the semilog plot technique, is justified. Furthermore, the other characteristic regimes can be analyzed to provide much more than just kh, S, and p^*, as illustrated below.

Double-Porosity Models

One frequently encountered type of heterogeneous response is double-porosity behavior, which is produced by fissured reservoirs. Two models of double-porosity behaviors have been studied[16-18,21]: one assumes pseudosteady-state interporosity flow; the other assumes transient interporosity flow. Both models are considered here, and the advantage of the derivative presentation in distinguishing various types of heterogeneous responses is shown.

Pseudosteady-State Interporosity Flow Model. The plots of the semilog slopes of examples are presented in Fig. 12.[17] For Example A, $\omega=1.0$, $\lambda e^{-2S}=3\times10^{-4}$, $(C_D e^{2S})_{f+ma}=10^{-1}$; and for Example B, $\omega=0.1$, $\lambda e^{-2S}=10^{-7}$, $(C_D e^{2S})_{f+ma}=10^{4}$. During the homogeneous regimes, the response follows a derivative $C_D e^{2S}$ curve, whereas at transition time, the flattening of the pressure behavior is changed into a very characteristic drop of the derivative. The transition regime is now described by two families of curves (Appendix A of Ref. 9): early transition is defined by the dimensionless group $(\lambda C_{Df+ma})/[\omega(1-\omega)]$ and late transition by $(\lambda C_{Df+ma})/(1-\omega)$. If the storage effect is present at the start of the transition (Example B), the response deviates from the corresponding $(\lambda C_{Df+ma})/[\omega(1-\omega)]$ curve (1.11×10^{-2} in this case), but storage being over at late transition times, the match on $(\lambda C_{Df+ma})/(1-\omega)$ (1.11×10^{-3}) is good.

The double-porosity model illustrates the gain in sensitivity of the derivative approach. The flattening of the pressure response during transition is generally difficult to identify on a log-log scale. In many cases, a semilog scale has to be used for refining the pressure curve match. With the derivative plot, the heterogeneous nature of the response is obvious, eliminating the need for any further plot for adjustments.

Table 2 contains field data from a pressure buildup recorded in a fissured formation. The derivative of pressure suggests the heterogeneous behavior, and the combined log-log plot of pressure and derivative (Fig. 13) is matched against the dual-porosity type curve of Ref. 17. The buildup curve shown was generated with the flow history before shut-in (multirate curve). The differential was taken as the slope of the superposition plot. The double-porosity model used provides a fairly good description of the response, despite the discrepancy during part of the transition. Results of analysis are presented in Appendix C.

Downloaded from http://onepetro.org/FE/article-pdf/4/02/293/2630137/spe-12777-pa.pdf/1 by Sandia National Laboratories user on 04 June 2025

TABLE 2—PRESSURE CHANGE vs. ELAPSED TIME
$p(\Delta t = 0) = 7{,}248$ psig

Run	Elapsed Time (hours)	Pressure Change
1	7.42509×10^{-4}	28.142
2	1.76790×10^{-3}	74.160
3	3.81868×10^{-3}	114.11
4	5.35677×10^{-3}	150.13
5	6.38216×10^{-3}	179.28
6	8.43294×10^{-3}	204.14
7	9.45833×10^{-3}	225.70
8	1.04837×10^{-2}	242.58
9	1.25345×10^{-2}	258.00
10	1.40726×10^{-2}	271.93
11	1.50980×10^{-2}	283.70
12	1.71488×10^{-2}	294.65
13	1.81741×10^{-2}	304.64
14	1.91995×10^{-2}	313.42
15	2.12503×10^{-2}	321.66
16	2.27884×10^{-2}	329.22
17	2.38138×10^{-2}	336.04
18	2.58646×10^{-2}	342.39
19	2.68900×10^{-2}	247.96
20	2.79154×10^{-2}	353.53
21	2.99661×10^{-2}	358.87
22	3.15042×10^{-2}	363.32
23	3.25296×10^{-2}	367.77
24	3.45804×10^{-2}	372.09
25	3.56058×10^{-2}	375.67
26	3.66312×10^{-2}	379.26
27	3.86820×10^{-2}	382.78
28	3.97074×10^{-2}	385.71
29	4.12454×10^{-2}	388.64
30	4.32962×10^{-2}	391.55
31	4.43216×10^{-2}	393.86
32	4.63724×10^{-2}	396.18
33	4.73978×10^{-2}	398.49
34	4.84232×10^{-2}	400.81
35	5.04740×10^{-2}	402.88
36	5.20120×10^{-2}	404.65
37	6.94437×10^{-2}	420.94
38	8.68753×10^{-2}	429.52
39	0.10379	434.51
40	0.12123	438.63
41	0.13968	441.76
42	0.15711	444.36
43	0.17455	446.48
44	0.19198	448.61
45	0.20941	450.10
46	0.22684	451.36
47	0.24427	452.63
48	0.26170	453.89
49	0.34938	457.50
50	0.43705	460.77
51	0.52420	462.94
52	0.61188	464.77
53	0.69955	467.72
54	0.78670	468.17
55	0.87438	468.67
56	0.96153	469.61
57	1.0492	470.22
58	1.1369	470.78
59	1.2240	471.27
60	1.3117	471.74
61	1.3994	472.18
62	1.4865	472.88
63	1.5742	473.88
64	1.6614	474.81
65	1.7490	475.72
66	1.8367	477.85
67	1.9239	478.63
68	2.0115	478.52
69	2.0997	478.98
70	2.1869	479.75
71	2.2745	480.50
72	2.3617	481.23

TABLE 2—PRESSURE CHANGE vs. ELAPSED TIME
$p(\Delta t = 0) = 7{,}248$ psig (continued)

Run	Elapsed Time (hours)	Pressure Change
73	2.4494	481.91
74	2.5370	482.57
75	2.6242	483.23
76	2.7119	483.89
77	2.7995	484.53
78	2.8867	485.14
79	2.9744	485.74
80	3.0615	486.35
81	3.1492	486.98
82	3.2369	487.58
83	3.3240	488.17
84	3.4117	488.74
85	3.4994	489.28
86	3.5865	489.83
87	3.6742	490.40
88	3.7614	491.48
89	4.1115	493.07
90	4.5494	495.59
91	4.9867	497.97
92	5.4240	500.33
93	5.8614	502.50
94	6.2997	504.71
95	6.7370	506.78
96	7.1744	508.65
97	8.0490	512.20
98	8.9242	515.47
99	9.7994	518.63
100	10.675	521.58
101	11.549	524.30
102	12.424	526.80
103	13.300	529.25
104	14.174	531.55
105	15.049	533.66
106	15.924	535.74
107	16.800	537.69
108	17.674	539.48
109	17.893	539.97
110	17.995	540.14
111	18.342	540.81
112	18.688	541.44
113	19.034	542.19
114	19.381	542.86
115	19.727	543.44
116	20.072	544.07
117	20.418	544.62
118	20.765	545.20
119	21.111	545.81
120	21.357	546.20
121	21.630	546.58
122	21.976	547.11
123	22.322	547.53
124	22.668	548.10
125	23.014	548.64
126	23.346	549.38
127	23.532	549.44
128	23.878	549.88
129	24.225	550.42
130	24.571	550.81
131	24.916	551.30
132	25.262	551.72
133	25.608	552.20
134	25.794	552.50
135	25.954	552.66
136	26.299	553.12
137	26.646	553.53
138	27.146	554.16
139	27.510	554.58
140	28.011	555.16
141	28.375	555.62
142	29.240	556.56
143	30.105	557.14
144	30.776	557.92

Downloaded from http://onepetro.org/FE/article-pdf/4/02/293/2630137/spe-12777-pa.pdf/1 by Sandia National Laboratories user on 04 June 2025

TABLE 2—PRESSURE CHANGE vs. ELAPSED TIME $p(\Delta t = 0) = 7{,}248$ psig (continued)

Run	Elapsed Time (hours)	Pressure Change
145	31.641	558.70
146	32.507	559.49
147	33.371	560.22
148	34.236	560.96
149	35.101	561.61
150	35.966	562.29
151	36.831	562.89
152	37.800	563.57
153	40.424	565.28

Flow History

Run	Duration (hours)	Flow Rates (STB/D)
1	3.0000	3945.0
2	1.5000	1265.0
3	1.7500	1470.0
4	6.7500	880.00
5	42.000	0.00000

Well and Reservoir Parameters

B	1.3
c_t, psi^{-1}	5×10^{-6}
h, ft	20
ϕ	0.08
μ, cp	1.3
r_w, ft	0.29

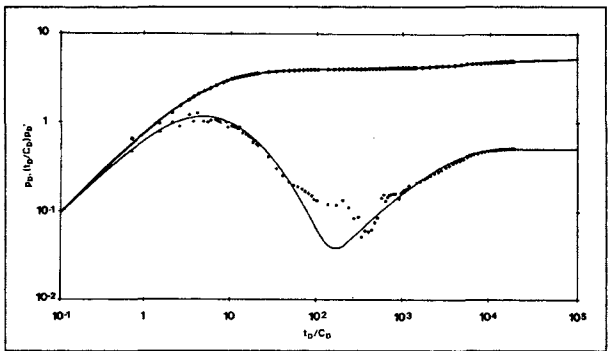

Fig. 13—Combined match of double-porosity data.

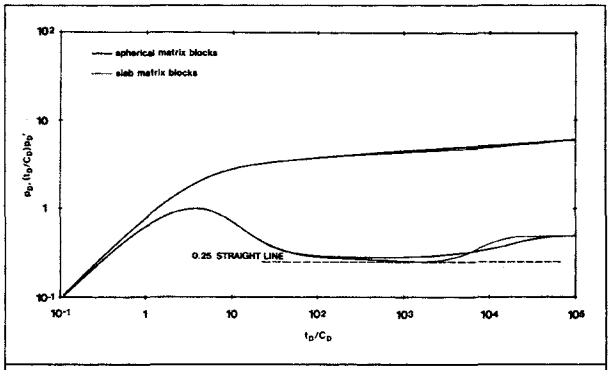

Fig. 14—Effect of block geometry on double-porosity responses (transient blocks to fissure flow).

Transient Interporosity Flow Model. The derivative response of the transient interporosity flow solutions is different from the pseudosteady-state curves: as for pressure, the derivative β' transition curves are obtained by displacing homogeneous $C_D e^{2S}$ curves by a factor of two along pressure and time axes.[19] The theoretical semilog straight line of the transition regime (slope one-half of true semilog) is then changed into a constant-derivative 0.25 line. On drawdown responses, the transient model does not show a derivative point below 0.25 during transition, as illustrated in Fig. 14.

Fig. 14 presents for the same parameters $(C_D e^{2S})_{f+ma} = 1$, $\beta' = 10^{-4}$, and $\omega = 10^{-2}$, the drawdown response produced by two matrix geometries, slabs and spheres. Though the pressure curves look identical, the derivatives are different; the sphere model response does not reach the 0.25 straight line but remains above it, whereas the slab curve is tangent to it but does not follow it for a significant duration.

For buildups, the derivative during transition regime may exhibit a lower value, down to 0.20, if the previous drawdown has not reached total system flow at shut-in time.[19] Similar distortions have been observed with a pseudosteady-state model.[17]

The discussion of the derivative curves of Fig. 14 illustrate the drawback of the method that consists of drawing intermediate straight lines on pressure plots. It is always possible to find several reasonably straight portions on a standard pressure curve plotted on any scale. This does not mean that an analysis of the intermediate-straight-line characteristics is justified. The derivative approach produces a zoom effect on small pressure changes and therefore can ascertain the presence of "straight-line behavior" and also give accurately its time limits.

The selection of the best solution between the double-porosity models, pseudosteady-state or transient interporosity flow, is generally straightforward; with the pseudosteady-state model, the drop of derivative during transition is a function of the transition duration. Long transition regimes, corresponding to small ω values, produce (Fig. 13) derivative levels much smaller than the practical 0.25 limit of the transient solution. An ambiguity might occur when the transition regime is of short duration. In such cases, pseudosteady-state curves (generated with a large ω value) can produce similar transient solutions, generated with a smaller ω value (on the order of 10^{-2} or 10^{-3} or less). Knowledge of the reservoir geology will help decide between the different fissure storage figures.

Cinco-Ley *et al.*[20] have shown that the pseudosteady-state behavior can be derived from the transient interporosity flow solution by adding a skin effect on the surface of the matrix blocks. It justifies *a posteriori* the use of two apparently different models for the description of fissured-formation responses. However, Cinco-Ley *et al.*'s theory suggests that the parameters obtained from the pseudosteady-state hypothesis (also called restricted interporosity flow), as defined originally by Warren and Root,[16] are not always applicable. In particular, λ should incorporate the matrix skin factor.[21] (Information on other well and reservoir configurations and other applications of the derivative of pressure are presented in Ref. 22.)

Conclusions

Transient test interpretation techniques have been reduced to the identification of characteristic regimes that produce a straight line when the pressure is plotted vs. time on various scales: radial flow with p vs. $\log(\Delta t)$, wellbore storage and pseudosteady-state with Δp vs. Δt, linear flow with Δp vs. $\sqrt{\Delta t}$, etc. With modern computing facilities, there is no reason to limit the pressure analysis to those restricted portions of the data during which a derivative is constant. Such types of data, corresponding to pure specific regimes, are often absent.

The method presented in this paper considers constant derivatives and changes of slope with a high definition. These transitional behaviors are ignored on conventional straight-line plots and are often featureless on log-log pressure-vs.-time graphs. A diagnosis is performed, with improved sensitivity, on the global response; the various flow regimes are identified, according to a logical chronology.

New analytical solutions are needed for general reservoir modeling to integrate characteristics neglected in traditional simplified solutions.

The conclusions are as follows:

1. The derivative approach improves the definition of the analysis plots and therefore the quality of the interpretation.
2. The differentiation of actual data has to be conducted with care to remove noise without affecting the signal. The derivative approach does not produce errors or noise but only reveals them.
3. The interpretation of pressure derivative is a single-plot procedure. If enough data are available, pressure and time matches are

Downloaded from http://onepetro.org/FE/article-pdf/4/02/293/2630137/spe-12777-pa.pdf/1 by Sandia National Laboratories user on 04 June 2025

fixed, so analysis is faster. This is important for real-time interpretation during well-test monitoring. Quick decisions during tests save rig time.

Nomenclature

B = FVF, RB/STB [res m^3/stock-tank m^3]
c_t = total compressibility, psi^{-1} [kPa^{-1}]
C = wellbore-storage constant, bbl/psi [m^3/kPa]
C_D = dimensionless storage constant
F_V = ratio of total volume of one porous system to bulk volume
h = formation thickness, ft [m]
k = permeability, md
K_0 = modified Bessel function, second kind, zero order
K_1 = modified Bessel function, second kind, first order
L = dimensionless distance on X axis of semilog analysis plot
m = absolute value of semilog straight-line slope, psi/cycle [kPa/cycle]
$m(p)$ = real gas potential, psi^2/cp [kPa^2/Pa·s]
p = pressure, psi [kPa]
p^* = extrapolated pressure
p_D = dimensionless pressure
$\bar{p}_D$ = Laplace transformed dimensionless pressure
p_i = initial reservoir pressure, psi [kPa]
Δp = pressure change, psi [kPa]
q = flow rate, STB/D [stock-tank m^3/d]
r_w = wellbore radius, ft [m]
s = Laplace space variable corresponding to t_D/C_D
s' = Laplace space variable corresponding to t_D
S = van Everdingen and Hurst skin factor
t_D = dimensionless time
t_p = production time
Δt = elapsed time, hours
X = time function
α = block shape parameter, ft^{-2} [m^{-2}]
β' = $\delta'[(C_De^{2S})_{f+ma}]/\lambda e^{-2S}$
γ = exponential of Euler constant (~ 1.78)
δ' = block shape factor (1.8914 for slab matrix blocks, 1.0508 for spherical matrix blocks)
θ = angle between two intersecting sealing faults
κ = ratio of permeability-thickness products
λ = pseudosteady-state interporosity flow parameter, $\alpha r_w^2(k_{ma}/k_f)$
μ = viscosity, cp [Pa·s]
ϕ = porosity of one system
ω = storativity ratio, $(\phi Vc_t)_f/[(\phi Vc_t)_f+(\phi Vc_t)_{ma}]=[(C_De^{2S})_{f+ma}]/(C_De^{2S})_f$

Subscripts

D = dimensionless
f = fissure
$f+ma$ = total system
i = point of interest
ma = matrix
M = match

Acknowledgments

We are grateful to the management of Flopetrol-Johnston for permission to publish this paper. Appreciation is also extended to A. Alagoa, B. Buchanan, G. Clark, M. Colvin, V. Kniazeff, and A. Tengirsenk for their assistance during this study. In particular, T. Whittle's (now with SSI) participation in this work and his very useful comments before finalization of the method are acknowledged.

References

1. Earlougher, R.C. Jr.: *Advances in Well Test Analysis*, Monograph Series, SPE, Richardson, TX (1977) **5.**
2. Horner, D.R.: "Pressure Build-Up in Wells," *Proc.*, Third World Pet. Cong., E.J. Brill, Leiden (1951) **11,** 503.
3. Ramey, H.J. Jr.: "Short-Time Well Test Data Interpretation in the Presence of Skin Effect and Wellbore Storage," *JPT* (Jan. 1970) 97–104; *Trans.*, AIME, **249.**
4. Agarwal, R.G., Al-Hussainy, R., and Ramey, H.J. Jr.: "An Investigation of Wellbore Storage and Skin Effect in Unsteady Liquid Flow: I. Analytical Treatment," *SPEJ* (Sept. 1970) 279–90; *Trans.* AIME, **249.**
5. Gringarten, A.C. *et al.*: "A Comparison Between Different Skin and Wellbore Storage Type Curves for Early-Time Transient Analysis," paper SPE 8205 presented at the 1979 SPE Annual Technical Conference and Exhibition, Las Vegas, Sept. 23–26.
6. Gringarten, A.C.: "Reservoir Limit Testing for Fractured Wells," paper SPE 7452 presented at the 1978 SPE Annual Technical Conference and Exhibition, Houston, Oct. 1–3.
7. Cinco-Ley, H. and Samaniego-V., F.: "Effect of Wellbore Storage and Damage on the Transient Pressure Behavior of Vertically Fractured Wells," paper SPE 6752 presented at the 1977 SPE Annual Technical Conference and Exhibition, Denver, Oct. 9–12.
8. Bourdet, D. and Gringarten, A.C.: "Determination of Fissure Volume and Block Size in Fractured Reservoirs by Type-Curve Analysis," paper SPE 9293 presented at the 1980 SPE Annual Technical Conference and Exhibition, Dallas, Sept. 21–24.
9. Bourdet, D., Ayoub, J.A., and Pirard, Y.M.: "Use of Pressure Derivative in Well Test Interpretation," paper SPE 12777 presented at the 1984 California Regional Meeting, Long Beach, April 11–13.
10. Bourdet, D. *et al.*: "A New Set of Type Curves Simplifies Well Test Analysis," *World Oil* (May 1983) 95–106.
11. Jain, A. and Ayoub, J.: "Pressure Build-Up in Gas-Lift Oil Wells, Falah Field, Offshore Dubai," *JPT* (March 1984) 466–74.
12. Agarwal, R.G.: "A New Method to Account for Producing Time Effect When Drawdown Type Curves are Used to Analyze Pressure Buildup and Other Test Data," paper SPE 9289 presented at the 1980 SPE Annual Technical Conference and Exhibition, Dallas, Sept. 21–24.
13. Tiab, D. and Kumar, A.: "Application of the p'_D Function to Interference Analysis," *JPT* (Aug. 1980) 1465–70.
14. Putigai, S.R. and Tiab, D.: "Pressure Derivative Type Curves for Vertically Fractured Wells," *SPEFE* (March 1988) 156–58; *Trans.*, AIME, **285.**
15. Al-Hussainy, R., Ramey, H.J. Jr., and Crawford, P.B.: "The Flow of Real Gases Through Porous Media," *JPT* (May 1966) 624–36; *Trans.*, AIME, **237.**
16. Warren, J.E. and Root, P.J.: "Behavior of Naturally Fractured Reservoirs," *SPEJ* (Sept. 1963) 245–55; *Trans.*, AIME, **228.**
17. Bourdet, D. *et al.*: "Interpreting Well Tests in Fractured Reservoirs," *World Oil* (Oct. 1983) 77–87.
18. Cinco-Ley, H., Samaniego-V., F. and Kucuk, F.: "The Pressure Transient Behavior for Naturally Fractured Reservoirs with Multiple Block Size," paper SPE 14168 presented at the 1985 SPE Annual Technical Conference and Exhibition, Las Vegas, Sept. 22–25.
19. Bourdet, D. *et al.*: "New Type Curves Aid Analysis of Fissured Zone Well Tests," *World Oil* (April 1984) 111–24.
20. Gringarten, A.C.: "Interpretation of Tests in Fissured and Multilayered Reservoirs with Double-Porosity Behavior: Theory and Practice," *JPT* (April 1984) 549–64.
21. de Swaan, A.: "Influence of Shape and Skin of Matrix-Rock Blocks on Pressure Transients in Fractured Reservoirs," paper SPE 15637 presented at the 1986 SPE Annual Technical Conference and Exhibition, New Orleans, Oct. 5–8.
22. Bourdet, D., Ayoub, J.A., and Pirard, Y.M.: "Supplement to SPE 12777, "Use of Pressure Derivative in Well-Test Interpretation," paper SPE 19215 available from SPE Book Order, Richardson, TX.
23. Cinco-Ley, H., Samaniego-V., F., and Viturat, D.: "Pressure Transient Analysis for High-Permeability Reservoirs," paper SPE 14314 presented at the 1985 SPE Annual Technical Conference and Exhibition, Las Vegas, Sept. 22–25.

Appendix A—Results of Analysis of Data, Table 1

Data are matched against the type curve for a well with wellbore storage and skin in a reservoir with homogeneous behavior. The match parameters are defined as $C_De^{2S}=4\times10^9$, pressure match $(p_D/\Delta p)_M=1.79\times10^{-2}$ psi^{-1}[0.26×10^{-2} kPa^{-1}], and time match $[(t_D/C_D)/\Delta t]_M=14.8$ $hours^{-1}$.

It follows as detailed in Ref. 10: $kh=[141.2qB\mu(p_D/\Delta p)_M]=$ 1,165 md-ft [355 md·m], $C=\{0.000295(kh/\mu)[\Delta t/(t_D/C_D)]_M\}=$ 9.3×10^{-3} bbl/psi [0.21×10^{-3} m^3/kPa], and $S=[0.5\ \ln(C_De^{2S}/C_D)]=7.7$.

Appendix B—Summary of the Differentiation Algorithms Considered

Three different approaches can be used. Smoothing is applied either on pressure data before differentiation (Algorithms A and B), on the derivative curve (Algorithm B), or on a second or third derivative

Downloaded from http://onepetro.org/FE/article-pdf/4/02/293/2630137/spe-12777-pa.pdf/1 by Sandia National Laboratories user on 04 June 2025

(Algorithm C), before integration of the data to produce the first derivative response.

Algorithm A fits a polynomial through data points around the point of interest and takes the exact polynomial derivative. The user can define the length of the time interval and the number of points for the polynomial fit. The degree of the polynomial could be varied by modifying the source program. Although this procedure smooths the data before differentiation, it generally works for actual data, provided that an adjustment of the polynomial degree is made to suit each particular case. Consequently, its use is cumbersome. In addition, the shape of the original derivative is affected.

Algorithm B uses a set of parabolas, each defined by three points of the vicinity of the point considered. The triplets are chosen as evenly spaced as possible. According to the "quality" of the data, 5 or more than 15 surrounding points participate in the calculation of each local derivative, which is an average of the derivative of the parabolas used. The smoothing is obtained by averaging pressure data and/or pressure derivative over a given time interval. This algorithm fails to reduce the noise effect sufficiently, even with large smoothing, which affects the original shape of the type curve.

Algorithm C calculates up to the third derivative for evenly spaced points, smooths it, and then integrates to obtain the final value of the first derivative. It tends to create false continuous oscillations at late times during infinite-acting radial flow.

Other smoothing techniques have been proposed,[23] but the algorithm presented in this paper was chosen for its simplicity and its efficiency at smoothing data with low distortion effects and because it is independent of the density of points. The same effect can be applied to actual data and to theoretical curves.

Appendix C—Results of Analysis of Data, Table 2

Data are matched against the type curve for a well with wellbore storage and skin in a reservoir with double-porosity behavior and pseudosteady-state interporosity flow. The match parameters are defined as $C_De^{2S}=1.1$, $\omega=0.015$, $\lambda e^{-2S}=4\times10^{-4}$, pressure match $(p_D/\Delta p)_M=8.72\times10^{-3}$ psi^{-1} [1.26×10^{-3} kPa^{-1}], and time match $[(t_D/C_D)/\Delta t]_M=370$ hours^{-1}.

It follows that $kh=[141.2qB\mu(p_D/\Delta p)_M]=1{,}830$ md-ft [558 md·m], $C=\{0.000295(kh/\mu)[\Delta t/(t_D/C_D)]_M\}=0.001$ bbl/psi [23×10^{-6} m^3/kPa], $S=[0.5\ \ln(C_De^{2S}/C_D)]=-3.6$, $\omega=0.015$, and $\lambda=2.9\times10^{-7}$. The extrapolated reservoir pressure was evaluated at $p^*=7{,}843$ psig [54.1 MPa].

SI Metric Conversion Factors

bbl	× 1.589 873	E−01	=	m^3
cp	× 1.0*	E−03	=	Pa·s
ft	× 3.048*	E−01	=	m
md	× 9.869 233	E−04	=	μm^2
psi	× 6.894 757	E+00	=	kPa
psi^{-1}	× 1.450 377	E−01	=	kPa^{-1}

*Conversion factor is exact.

SPEFE

Original SPE manuscript received for review April 14, 1984. Paper accepted for publication April 28, 1988. Revised manuscript received March 7, 1989. Paper (SPE 12777) first presented at the 1984 California Regional Meeting held in Long Beach, April 11–13.

SPE 19215, "Supplement to SPE 12777, Use of Pressure Derivative in Well-Test Interpretation," available from SPE Book Order Dept.

Downloaded from http://onepetro.org/FE/article-pdf/4/02/293/2630137/spe-12777-pa.pdf/1 by Sandia National Laboratories user on 04 June 2025